ABSTRACT

Title of Thesis: PROPERTIES OF A DTN PACKET FORWARDING SCHEME INSPIRED BY THERMODYNAMICS

Bipin Mathew, Master of Science, 2010

Thesis directed by: Professor Richard Hyong-Jun La
Department of Electrical and Computer Engineering

In this thesis, we develop a discrete time model of a recently proposed algorithm, inspired by thermodynamics, for message routing in Disruption Tolerant Networks (DTNs). We model the evolution of the temperature at the nodes as a stochastic switched linear system and show that the temperatures converge in distribution to a unique stationary distribution that is independent of initial conditions. The proof of this result borrows tools from Iterated Random Maps (IRMs) and Queuing theory. Lastly, we simulate the proposed algorithm, using a variety of mobility models, in order to observe the performance of the algorithm under various conditions.

PROPERTIES OF A DTN PACKET FORWARDING SCHEME INSPIRED BY THERMODYNAMICS

by

Bipin Mathew

Thesis submitted to the Faculty of the Graduate School of the
University of Maryland, College Park in partial fulfillment
of the requirements for the degree of
Master of Science
2010

Advisory Committee:
Professor Richard Hyong-Jun La, Chair/Advisor
Professor Armand Makowski
Professor Sennur Ulukus

Table of Contents

List of Figures

Chapter 1

Introduction

1.1 Background

Disruption Tolerant Networks (DTNs) refer to network architectures that are tolerant of sparse connectivity and long delays between the availability of links from sources to destinations. The connectivity of the network may be impacted by limited wireless radio range, sparsity of mobile nodes, energy resources, noise and adversarial attack. Research into DTNs has been motivated by applications including the deployment of resources into remote, hostile or dangerous environments, such as a battlefield or post-disaster areas, and to improve communication in inherently sparse environments, such as remote villages or deep-space. Disruptive environments provide unique challenges to routing protocols, which do not exist in other regimes. For example, protocols that rely on establishing end-to-end connectivity, e.g., TCP, AODV and DSR are ill suited to disruptive environments [4]. Since the establishment of a connection requires at least one round-trip between the sender and the receiver, if the round-trip delay exceeds the duration of any link in the network, no data may flow at all. Even if a momentary connection is established, frequent link breaks, which are a characteristic of DTNs, will result in a flood of route maintenance messages, in the case of AODV and DSR, and anemic throughput rates in the case of TCP. Since persistent routes from sources to destinations

are rare, DTN networks must use a "Store-Carry-Forward" routing methodology – storing both its own packets as well as those from other nodes and forward them on to still other nodes opportunistically. To ameliorate the effect of long latencies on the application layer, DTN packets usually encapsulate enough data to allow the application layer to proceed with a meaningful unit of work while waiting for further packets. For this reason, packets in DTN networks are normally larger than their counterparts in conventional networks and are often termed *bundles*. Combined, these two factors necessitate much larger buffers, and much more intelligent buffer management, than is normally available in conventional routers.

In response to these issues, numerous DTN routing algorithms have been proposed in the literature. A basic taxonomy of these algorithms divide them along two axes: the first is the degree to which replication of bundles is used, and the second is the extent to which the algorithm uses history to glean insights into the topology and dynamics of the network. A third axis would be the expected a-priori predictability of the one-hop connectivity of the network, which can vary widely from largely unpredictable (e.g., wildlife tracking), to semi-predictable (e.g., transportation networks) to completely predictable (e.g., space-communications). In this thesis, we shall exclude discussion of the completely predictable case. When connectivity is completely predictable, it is possible to formulate a linear program to route packets optimally, in the sense of minimum delay, with connectivity and bandwidth constraints. Details can be found in [7].

In this thesis we shall be studying the convergence properties of a parameter, called temperature, under a DTN routing algorithm recently proposed by Kalantari

and La [10] which is motivated by thermodynamics. In general outlines, to each node is associated a notional temperature based on its exposure to a one or more sink nodes. Sink nodes are the nodes to which packets are to be delivered and are maintained at a constant temperature. There are two application domains that need to be distinguished. The first is when the objective is to route packets to one or more sink nodes; in a sense, for packets to be pulled towards any one of several sink nodes. On can visualize, for example, routing packets to any one of several access points or hubs. The second possibility is that packets need to be routed from the source node to a *particular* destination, that may be different from packet to packet, and source node to source node. In both cases, when two nodes come in contact, meaning they can communicate with each other, they transfer heat between themselves using standard laws of thermodynamics. In the first case, each node maintains a single scalar temperature that measures its direct and indirect exposure to the collection of sink nodes to which packets need be delivered. The nodes then opportunistically transfer these packets to ever warmer nodes until, eventually, they are delivered to one of the sink nodes. In the second case, one can imagine replicating this same approach for each destination. In this case, each node will maintain an array of temperatures, one entry per destination, and viz-a-viz measure the nodes direct and indirect exposure to that particular destination.

The thesis is organized as follows: In the next section, we shall provide a brief survey of current state of the art in DTN routing protocols. In Chapter 2, the proposed algorithm is described with the formalism necessary for analysis. Section 2.2 of the chapter will present our results regarding the convergence properties of

the temperatures under the algorithm for various connectivity models. In Chapter 3, we shall see the algorithm in action through various simulations using standard mobility models ; Chapter 4 concludes the thesis with a discussion of future work and other properties that might be of interest.

1.2 Literature Survey

The simplest routing algorithms for DTN networks are *direct delivery* and *epidemic routing* [20]. As the name suggests, direct delivery transfers messages directly between the source and the destination, relying entirely on the mobility of each node. epidemic routing, also known as *Flooding*, in contrast, forwards all non-duplicated messages, including its own, to every node it encounters – eventually delivering its messages to the appropriate destinations. direct delivery and epidemic routing represent two extremes and illustrate a natural trade-off in DTN networks; suppose, for the purpose of illustration, that there are M nodes in the network, that messages are N bytes long, and that they can be delivered in their entirety during the contact times between nodes. Direct delivery would use only N bytes of bandwidth and minimum buffer space since only its own messages are stored and the message is transferred only once. However, since delivery depends on the source and the destination eventually meeting, packets may never be delivered or may experience long latencies. epidemic routing, on the other hand, forwards all its messages to intermediaries conceivably using $N(M-1)$ bytes of bandwidth to transfer data in addition to the auxiliary information exchanged during encounters

to determine which packets are non-duplicated and ready for transfer. In addition to bandwidth, large buffers may be required to store in-transit packets to achieve minimum latency.

Most practical algorithms seek a compromise between these extremes. These approaches rely on limiting replications within the network, more intelligently coding the messages, using heuristics to gain insight into the topology and dynamics of the network or using a combination of these methods. The simplest of the practical algorithms is *simple replication*. In this approach, the source node copies its message to the first r intermediaries it encounters. These intermediaries then use direct delivery to deliver the message to the intended destination. Using this approach the r redundant copies reduce the expected latency of the network while using only rN bytes of bandwidth. We see that if $r = 0$ this method is equivalent to direct delivery, and as r gets larger, it behaves more like epidemic routing. A variant of this technique proposed in the literature is *binary spray and wait* [17]. In this approach, instead of the source node distributing a single copy of the message to the first r intermediaries it encounters, binary spray and wait didactically transfers $r/2^k$ copies of the message to the k^{th} intermediary it encounters which does not already possess the message, where $k \in 1, ..., \log r$. When only a single copy of the message remains, the source node switches to direct delivery. Each of the intermediary nodes, likewise, employ the same scheme with its copies of the message; repeatedly transferring half its store of messages to other intermediary nodes, without a copy of the message. It was shown that, when node movements are independent and identically distributed (i.i.d), binary spray and wait has the minimum expected delay among all simple

replication-based algorithms.

An alternative to simple replication of packets is to use erasure codes [21]. Borrowed from the Information Theory literature, erasure codes were originally designed for error correction in the binary erasure channel; a popular example is the Reed-Solomon codes used in the encoding of compact audio disks. Erasure codes transform a message of size M into a larger coded message of size rM where r is the replication factor. This larger coded message is subsequently divided into a large number, b, of blocks each of size rM/b. The defining feature of these codes is that the original message can be recovered as long as $1/r$ of the blocks are recovered. This feature may be exploited in the design of DTN networks to distribute the responsibility of delivering a particular message over a larger number of nodes for the same aggregate bandwidth. To be more precise, erasure coding based algorithms evenly distribute the b code blocks among the first kr relay nodes, where k is some integer constant. The aggregate bandwidth of erasure code based algorithms is the same as simple replication since each of the kr relay nodes carry only $rM/b \times b/kr = M/k$ bytes of data. However, in contrast to simple replication where only one of the r replicas of the message is required to decode the message at the sink, erasure code based algorithms require that at least k of the kr relays deliver their packets. The merits of erasure codes over simple replication become significant when the number of low latency relays is large in comparison to r. In fact, it was shown in [21] that the expected delay, when the delay of each relay in delivering its packets is independent with common distribution function F, approaches the constant $\zeta_{1/r}$ as the number of nodes $n = kr$ gets large, where $\zeta_{1/r}$ is the $\frac{1}{r}^{th}$ quantile of the delay distribution

F.

History based approaches seek to gain inferences into the dynamics of the network to better facilitate packet delivery. Two examples of this approach that have been deployed in the field are MaxProp [3] and ZebraNet [9]. ZebraNet is an ad-hoc wireless network designed for the tracking of zebras in Kenya. Wireless transmitters are affixed to zebras to record their movements in the wild via GPS. These positions are to be eventually collected at a central stationary base station. Since zebras herd over thousands of kilometers and with the possibility of theft or vandalism, the use of cellular or wireless towers was not an option. The history based algorithm used in this network seeks to selectively route messages to intermediary zebras more likely to encounter the base station. This is done via the concept of *Hierarchy Levels* – a notional number that corresponds to the zebras' frequency of contact with the base station. The transceivers attached to the zebras periodically scan its surroundings for opportunities to either deliver its messages to the base station or transfer them to intermediary nodes. In lieu of an opportunity to deliver its messages to the base station, zebras transfer their messages to the intermediary with the highest Hierarchy Level (HL) within contact range. If a node remains out of contact with the base station, its HL is decremented by one for every D consecutive scans that the base station remains out of range, where D is a tunable parameter. Conversely, For each scan where the base station is detected, the transceiver delivers its queue of messages and increments its HL by one. ZebraNet also employs a simple buffer management system wherein to make room for new packets, each node first deletes the oldest messages in its queue not originated by that node, followed by its own

oldest messages. In this way, ZebraNet preferentially propagates newer messages over older ones in the network. It was found by the authors, in a simulation which mimicked zebra migrations, that over a broad range of radio ranges, this history based method outperformed both direct delivery and epidemic routing schemes in bandwidth and storage constrained scenarios.

MaxProp takes a different and more involved history-based approach. In the core algorithm, each node maintains a buffer of messages sorted by a *Delivery Likelihood* (DL) metric that corresponds to the nodes ability to deliver messages, possibly through intermediaries, to a specified destination d. During transfer opportunities, the packets with the highest DL are transferred first while packets with the lowest DL are the first to be deleted to make room for newer packets. The DL of a packet with a particular destination is estimated in the following manner: each node i maintains a vector of values f_j^i that successively estimates the probability that node j will be in range during the next scan. For all nodes f_j^i is initially set to $1/\left(|N|-1\right)$. Every time a node j comes into range of node i, the value of f_j^i is incremented by 1 and the entire vector f^i is renormalized to sum to 1. During encounters nodes opportunistically transfer their messages as well as these vectors. To each path from node i to destination d can be associated a cost $c\left(i, i+1, ..., d\right)$ that correlates to that paths average availability. In the MaxProp approach this cost is calculated as the sum of the probabilities that each link along the path does not exist, i.e.,

$$c\left(i, i+1, ..., d\right) = \sum_{x=i}^{d-1} \left[1 - \left(f_{x-1}^{x}\right)\right] \tag{1.1}$$

The DL of node i to deliver messages to node d is then the minimum over all possible paths of the above expression. This can be computed efficiently using a modified version of Dijkstra's algorithm; since the cost monotonically increases in the number of links, a depth-first search of the paths can terminate once its cost exceeds that of the current best path. Again, it was found empirically that the core algorithm disadvantaged newer packets in the network, and a modification was proposed wherein if the hop-count of an incoming packet was below a threshold, T, it was enqueued and given priority in the queue by hop-count, while for already enqueued packets with hop-count greater than T they are prioritized by the DL. A diagram representing this approach is shown in figure (1.1). It was shown within reference [3] that the MaxProp algorithm exhibits superior performance, in terms of both delivery rate and latency in comparison to both random routing, where a random message from the queue is forwarded at each opportunity, and an Oracle based Dijkstra algorithm, where future connectivity is known with certainty. This is so, since even though future connectivity is known, the oracle is not aware of buffer space and link bandwidth allocations of all peers at all times in the future. A truly globally optimal routing algorithm where buffer space, bandwidth and traffic load are all taken into consideration becomes an NP-complete problem which can be solved via a dynamic programming algorithm as in [7].

In addition to these "pure" methods, it is also possible to combine them in various ways. For example, it is possible to combine a history based metric with simple replication or erasure coding to improve performance. An example of a combined approach that has been suggested in the literature is Estimation-Based Erasure-coding

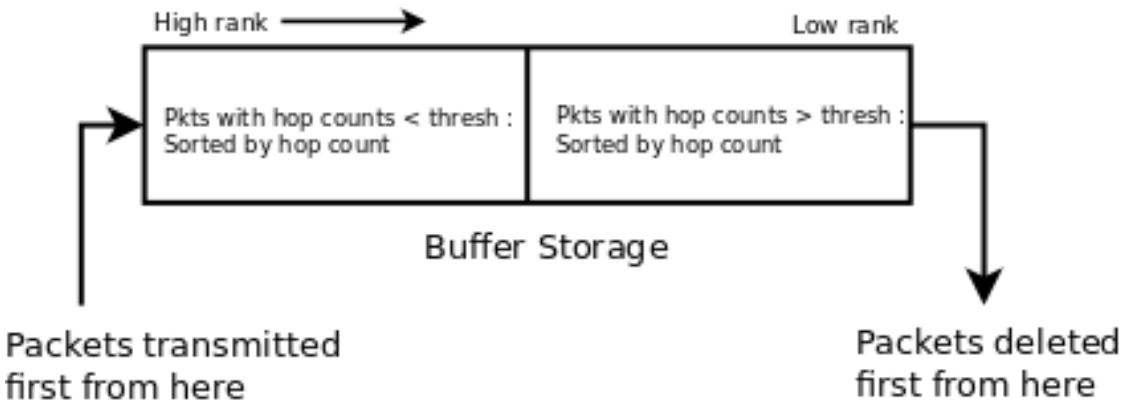

Figure 1.1: Buffer management using the MaxProp routing protocol.

[12] (EBEC). Like the basic erasure coding method, messages are transformed into a large number of coded packets. However, instead of being forwarded to the first rk intermediaries, they are forwarded in proportion to their Average Contact Frequency (ACF) with the desired destination node. The ACF, $\tau_{i,j}$, of node i with j is defined as the number of encounters between these nodes i and j over a predefined time interval T, i.e., $\tau_{i,j} = N_{i,j}/T$ where $N_{i,j}$ is the number of encounters between nodes i and j in time T. The dispersal of packets corresponding to a particular message by nodes in the network is divided into two states: a spreading state and a forwarding state, depending, respectively, on whether the number of packets held by that node is greater than or less than a threshold G. To illustrate, let node A be an intermediary carrying m_A packets destined for node D. In the spreading state, when $m_A > G$, if node A encounters node B, node A will transfer $m_B = m_A \frac{\tau_{B,D}}{\tau_{A,D}+\tau_{B,D}}$ messages to node B and retain $m_A - m_B$ packets. It is presumed that node B does not already have packets corresponding to this message for node D, in which case it will not participate in this exchange. In the forwarding state, when $m_A \leq G$, node A

on encountering a node B with an ACF greater than its own for destination D will transfer *all* its messages to node B. Since a message can be reconstructed as soon as k packets are delivered, it is unnecessary for an intermediary to retain more than k packets. Therefore, the threshold is set so that $G \leq k$. The authors evaluated the EBEC algorithm along side binary spray and wait as well as conventional erasure coding using a random waypoint model on discrete locations, and the EBEC was found to outperform both of them in terms of delivery latency.

An unbiased evaluation of these various approaches and combinations of approaches is attempted in [6]. Therein these algorithms were benchmarked against simulations derived from three popular real-world mobility traces; in ascending order of connectivity: The MIT Bluetooth trace (MITBT), the IBM Access Points Trace (IBM) and the MIT Cell Towers trace (MIT). In addition to the diversity of connectivity present in these traces, the available bandwidth along these links were also varied from low (100 KiB/s), medium (1000 KiB/s) to high (10,000 KiB/s), thus breaking down the simulation space into to nine categories. It was found that in terms of delivery rate, Flooding and Perfect Oracle dominated under weak connectivity while MaxProp performed well under high connectivity. MaxProp however, could not take advantage of higher available bandwidth, delivering about the same amount of data even as bandwidth was increased 100 fold.

Chapter 2

A DTN Routing Algorithm Inspired by Thermodynamics

2.1 Basic Model and Assumptions

Consider a set $\mathcal{N} = \{1, 2, \cdots, m\}$ of mobile nodes moving in some domain $\mathbb{D}$, which is a subset of $\mathbb{R}^2$. The mobility of the nodes is allowed to be heterogeneous; the speed and support or range of the mobility may differ from one node to another. The location of node $i \in \mathcal{N}$ at time $t \geq 0$ is denoted by $L_i(t)$, and the trajectory of node i is given by $\mathbb{L}_i = \{L_i(t); t \in \mathbb{R}_+\}$ where $\mathbb{R}_+ = [0, \infty)$. Each node is assumed to generate messages that arrive according to some stochastic process, and that these messages are destined for a single source node. Without loss of generality, we may assume that the sink node is node 1.

We assume that a pair of nodes can communicate with each other through a wireless communication link if and only if their distance is smaller than or equal to a fixed communication range of the nodes, which we denote by $\beta > 0$. Due to the mobility of the nodes, the link between two nodes, say i and j, is dynamically set up and is torn down based on the time-varying distance between them. We can model the one-hop connectivity between two nodes i and j, $i \neq j$, using an on-off process $\mathbb{C} = \{C_{ij}(t); t \in \mathbb{R}_+\}$, where

$$C_{ij}(t) = \begin{cases} 1 & \text{if } ||L_i(t) - L_j(t)||_2 \leq \beta \\ 0 & \text{otherwise} \end{cases} \tag{2.1}$$

where $||L_i(t) - L_j(t)||_2$ is the Euclidean distance between $L_i(t)$ and $L_j(t)$. When $C_{ij}(t) = 1$, we say that nodes i and j are in *contact* or *connected*. As mentioned previously, for DTNs, it is unlikely that there will be a long-lived end-to-end route available from a node to the sink. Therefore, the nodes must forward their messages to the sink in an opportunistic manner by relying only on intermittent links between nodes.

In practice, it is likely that the contact times (i.e, the amount of time two nodes spend in contact once they meet) are much larger than the amount of time needed to complete a transfer of messages. Hence, we assume that a transfer of messages occurs (almost) instantly and the nodes can complete all necessary transfer of messages while they remain in contact.

Our goal is to find a model that can capture the heterogeneous mobility of nodes and allows us to design a simple, yet efficient packet forwarding scheme that exploits the knowledge of nodes' mobility. This is achieved by introducing a time-varying measure that quantifies (direct or indirect) exposure of each node to the sink (over some period), which obviously depends on nodes' mobility and frequency at which they visit the sink. This measure can also be viewed as an estimate of nodes ability to forward messages to the sink (either directly or indirectly). It is used to guide packet forwarding decisions by the nodes when they meet. In a nutshell, when two nodes meet, messages are forwarded from the node with a smaller value to the

node with a larger value. The intuition behind this is that a node with a large value is believed to have more access to the sink. Again, this access may take the form of direct access when the node meets the sink or indirect access through other relay nodes.

We first list some properties one would expect such a measure to possess:

1. The value of the measure lies in a compact interval. Moreover, it increases monotonically while the node is in proximity of the sink, i.e., the sink is in contact with the node.

2. When a node moves out of the communication range of the sink, its value decreases monotonically while the node is not in contact with any other node.

3. While two nodes are within the communication range of each other, their values are continually updated; the value of the node with a larger (resp. smaller) value decreases (resp. increases).

The first two properties are intuitive. The last property can be motivated as follows: When a node i with a smaller value comes in contact with another node j with a larger value, loosely speaking, the encounter provides node i with an opportunity to relay some messages through node j, increasing node i's indirect access to the sink. This type of indirect access to the sink needs to be captured when multi-hop forwarding of messages is necessary. At the same time, as node i relies on node j to carry some of node i's messages as a relay node, node j's ability to serve as a relay node to other nodes should be discounted.

The measure proposed in [10] is to associate with each node i a temperature $\theta_i \in [0, T]$. The sink node is maintained at a temperature T. The temperature of the non-sink nodes then evolves according to standard thermodynamic laws first proposed by Newton. In other words, when two nodes are in contact, the rate at which the temperature changes is directly proportional to their difference in temperature. When a node is isolated, that is, not connected to any other node, it loses heat to the environment at a rate γ. This relationship may be expressed by a system of differential equations:

$$\frac{d}{dt}\theta_i(t) = \begin{cases} 0 & \text{if } i = 1, \\ -\gamma\theta_i(t) + \sum_{j \in C_i(t)} \lambda_{ij} \left(\theta_j(t) - \theta_i(t)\right) & \text{otherwise} \end{cases} \tag{2.2}$$

where $C_i(t) = \{j \in \mathcal{N} : C_{ij}(t) = 1\}$, i.e., the set of nodes that are in contact with node i at time t. In the rest of this thesis, we will assume that the coefficients of heat transfer between nodes are symmetric and identical, i.e. $\lambda_{ij} = \lambda_{ji} = \lambda$. This allows us to simplify the above system of equations as follows.

$$\frac{d}{dt}\theta_i(t) = \begin{cases} 0 & \text{if } i = 1, \\ -\left[\gamma + \lambda N_i(t)\right]\theta_i(t) + \lambda \sum_{j \in C_i(t)} \theta_j(t) & \text{otherwise,} \end{cases} \tag{2.3}$$

where $N_i(t) = |C_i(t)|$ is the number of nodes connected to node i at time t. As a linear system of differential equations, it is fruitful to think of the above as a matrix equation.

$$\frac{d}{dt}\theta(t) = A(t)\theta(t) \tag{2.4}$$

where $A(t)$ is a matrix of the form

$$A_{ij}(t) = \begin{cases} -(\gamma + N_i(t)\lambda) & \text{if } i = j \text{ and } i \neq 1, \\ \lambda & \text{if } i \neq j \text{ , } j \in C_i(t) \text{ and } i \neq 1, \\ 0 & \text{otherwise,} \end{cases}$$

As a device for understanding, it is useful to consider a typical instantiation of the above matrix. An example of one is shown below.

$$A(t) = \begin{pmatrix} 0 & 0 & \cdots & * & 0 & 0 \\ * & -(\gamma + N_2(t)\lambda) & \cdots & \lambda & 0 & * \\ \vdots & \vdots & \ddots & \vdots & \vdots & * \\ * & \lambda & \cdots & -(\gamma + N_j(t)\lambda) & 0 & * \\ 0 & 0 & \cdots & 0 & -\gamma & 0 \\ * & * & \cdots & * & 0 & * \end{pmatrix} \tag{2.5}$$

where the asterisk represents possibly non-zero entries. We observe that the first row is zero; the sink node is insulated from heat loss to the environment and other nodes. Another interesting feature is the fact that the $(1,1)$-submatrix, the matrix with the first row and the first column removed, is symmetric reflecting the fact that in our model the coefficients of heat loss are identical and symmetric. It will also be useful to note in the analysis that follows, that each off-diagonal entry where $A_{i,j}(t) = \lambda$, adds one to the value of $N_i(t)$ and $N_j(t)$. As a consequence, on any row j, the number of off-diagonal λ's will be $N_j(t)$.

To study the evolution of $\theta_i(t)$ in this setting requires a rather complicated apparatus of switched linear systems. Commonly, a stability analysis of such sys-

tems would entail finding a common quadratic Lyapunov matrix over all possible system matrices [19]. For the purposes of this paper, we shall study a discrete time approximation to this continuous time model. We will assume that there exists a minimum epoch of length h such that the connectivity of the nodes remains constant. In other words, $C(t)$, or equivalently, $A(t)$ is constant on all intervals of the form $[nh, (n+1)h)$ where $n = 0, 1, ...$ We let $C_n = C(t)$, $A_n = A(t)$ and $N_j^n = N_j(t)$ on the interval $[nh, (n+1)h)$. Over each of these intervals the evolution of the temperature vector, $\theta(t)$ is governed by the linear differential equation given in (2.4). We shall examine the temperature vector at the end points of these intervals; that is, with some abuse of notation, $\theta_n = \theta(nh)$. We can write an implicit relationship between consecutive θ_n as

$$\theta_{n+1} = \theta_n + \int_{nh}^{(n+1)h} A_n \theta(\tau)\, d\tau$$

Stated differently, the temperature vector evolves according to a linear, constant coefficient, differential equation (LCCDEs) over each time domain. LCCDE's have an extensive history and literature [16] and it is well known that the explicit solution can be written as

$$\theta_{n+1} = e^{A_n h}\theta_n \tag{2.6}$$

where $e^{A_n h}$ is the matrix exponential defined by the following infinite series.

$$e^{A_n h} = \sum_{k=0}^{\infty} \frac{A_n^k h^k}{k!}$$

It can be shown that this series converges uniformly and absolutely on any interval $[-h, h]$ where $h > 0$ is arbitrary.

In our analysis, we will make extensive use of an alternative formulation of the matrix exponential that can be motivated in a heuristic manner similar to the derivation of the exponential for scalars. Suppose that a interval $[t_n, t_{n+1}]$ is divided into N segments, each of length $(t_{n+1} - t_n)/N$. Setting $h = t_{n+1} - t_n$ and using equation (2.4) we can write a first order approximation to the differential equation over each segment as follows.

$$\begin{aligned} \theta\left(t_n + (k+1)\frac{h}{N}\right) &\approx \theta\left(t_n + k\frac{h}{N}\right) + A_n\theta\left(t_n + k\frac{h}{N}\right)\frac{h}{N} \\ &\approx \left[I + A_n\frac{h}{N}\right]\theta\left(t_n + k\frac{h}{N}\right) \end{aligned}$$

where $k \in \{0, \ldots, N-1\}$. Expanding this recursion, the approximation becomes exact as $N \to \infty$.

$$\theta(t_{n+1}) = \lim_{N\to\infty}\left[I + A_n\frac{h}{N}\right]^N \theta(t_n)$$

Then, over each interval $[nh, (n+1)h]$ we can write, setting $t_n = nh$ and $t_{n+1} = (n+1)h$, that

$$\theta_{n+1} = \lim_{N\to\infty}\left[I + A_n\frac{h}{N}\right]^N \theta_n$$

Setting corresponding terms equal we would expect that

$$e^{A_n h} = \lim_{N\to\infty}\left[I + A_n\frac{h}{N}\right]^N \tag{2.7}$$

we recognize the similarity of this expression to the standard definition of the scalar exponential function. This heuristic argument can be made rigorous and a full proof is provided in appendix A.

2.2 Convergence in Distribution

In this section we will show that the temperature vector θ_n converges in distribution under the dynamical model described by equation (2.6). We will do this by establishing the stronger condition that the iteration converges in norm, i.e. that there exists a random vector Θ such that $||\theta_n - \Theta|| \to 0$. In the process, we will make use of results obtained in the study of *Iterated Random Maps* (IRMs). IRMs are any iteration of the form $\theta_{n+1} = f(\theta_n, A_n)$ where $\{A_n; n \geq 1\}$ is a random process. IRMs are an area of active research and have found applications in numerous fields, including the generation of fractal images [5], queuing theory [14] and stochastic optimization [13].

In the following analysis we will initially assume that the random process $\{A_n; n \geq 1\}$ is independent and identically distributed (i.i.d) and later extend the result to the more general class of stationary random processes. In both cases, the underlying state space Ξ is constructed in the following manner: Suppose there are M nodes and let Ξ be the set of all $2^{\binom{M}{2}}$ possible one-hop connectivity graphs. To each graph $\xi \in \Xi$, there corresponds a unique connectivity matrix C_ξ and heat transfer matrix A_ξ and to each state also corresponds a probability p_ξ. With some abuse of notation we will let Ξ indicate the set of graphs, connectivity matrices, or

heat transfer matrices interchangeably based on context.

2.2.1 The Independent Identically Distributed Case

The convergence of IRMs in the i.i.d setting center on establishing that the ensemble of maps $f_\xi(x) = \{e^{A_\xi h}x : \xi \in \Xi\}$ contract *on average*, in a sense to be described below. A map f_ξ over a metric space $(S, \|\cdot\|)$ is a contraction mapping, if there exists a non-negative constant $K_\xi < 1$, such that

$$||f_\xi(x) - f_\xi(y)|| \leq K_\xi||x - y|| \text{ for all } x, y \in S. \tag{2.8}$$

In our particular case, S will be the set of all vectors in $x \in \mathbb{R}^M$, in which x_1 is equal to T – the fixed temperature of the sink node, i.e., $S = \{x \in \mathbb{R}^M : x_1 = T\}$. We will show, through a series of lemmas, that for any choice of $\xi \in \Xi$, f_ξ forms a contraction mapping on S.

Lemma 2.2.1. *for any matrix $A_\xi \in \Xi$ and $h > 0$, $e^{A_\xi h}$ is element-wise non-negative.*

Proof. (Lemma 2.2.1) In the previous section, we established that,

$$e^{A_\xi h} = \lim_{N\to\infty}\left(I + A_\xi\frac{h}{N}\right)^N$$

Expanding the base of the exponent on the right hand side, we observe that

$$I + A_\xi\frac{h}{N} = \begin{cases} 1 & \text{if } i = j = 1 \\ 1 - \frac{h}{N}(\gamma + |C_\xi|\lambda) & \text{if } i = j \text{ and } i \neq 1 \\ \frac{h}{N}\lambda & \text{if } i \neq j \text{ , } j \in C_\xi \text{ and } i \neq 1 \\ 0 & \text{otherwise} \end{cases}$$

It is clear that regardless of h we can select an N large enough such that this matrix is element wise positive - namely when $N > h(\gamma + M\lambda) \geq h(\gamma + \lambda \max_{k \in 1 \cdots M}\{N_k\})$ where M is the number of nodes. The lemma follows since a product of positive matrices is non-negative. □

Lemma 2.2.2. *For any A_ξ, $f_\xi(x) = e^{A_\xi h}x$ forms a contraction mapping on the metric space $(S, ||\cdot||_\infty)$, where $||x||_\infty$ is the ∞-norm, defined as $||x||_\infty = \max_i |x_i|$.*

Proof. (Theorem 2.2.2) We begin the proof by finding an upper-bound for the expression

$$||e^{A_\xi h}x - e^{A_\xi h}y||_\infty = ||e^{A_\xi h}(x - y)||_\infty \tag{2.9}$$

since $x, y \in S$ it is clear that $x_1 - y_1 = 0$ is zero. Moreover, since $\left[e^{A_\xi h}\right]_{1,j} = 0$ for $j > 1$, we see that the value of the above norm is unchanged if we restrict ourselves to considering only the norm of the product of the $(1,1)$-submatrix of $e^{A_\xi h}$ (the matrix with the first row and the first column removed) and the last $M-1$ terms of $x-y$. Let us designate these as $\tilde{e}^{A_\xi h}$ and $||\tilde{x}-\tilde{y}||$ respectively. It is also easy to show that $\tilde{e}^{A_\xi h} = e^{\tilde{A}_n h}$ where $\tilde{A}_\xi$ is the $(1,1)$-submatrix of A_ξ. Using these observations we can rewrite equation (2.9) as

$$||e^{A_\xi h}x - e^{A_\xi h}y||_\infty = ||e^{\tilde{A}_\xi h}(\tilde{x} - \tilde{y})||_\infty$$

It is possible to bound this quantity by making use of the induced matrix norm. The induced matrix norm corresponding to the ∞-norm for vectors is the maximum of the sum of the absolute values of the rows, i.e., for a matrix $||A||_\infty =$

$\max_{i\in 1\ldots M}\sum_{j=1}^{M}|A_{ij}|$. It is a property of matrix norms that for square matrices A, B and vector x, $||AB||_\infty \leq ||A||_\infty||B||_\infty$ and $||Ax||_\infty \leq ||A||_\infty||x||_\infty$ [18]. Using these properties we can write the following sequence of inequalities.

$$\begin{aligned}
\|e^{A_\xi h}x - e^{A_\xi h}y\|_\infty &= \|e^{\tilde{A}_n h}\left(\tilde{x}-\tilde{y}\right)\|_\infty \\
&\leq \|e^{\tilde{A}_n h}\|_\infty \|\tilde{x}-\tilde{y}\|_\infty \\
&\leq \left\|\lim_{N\to\infty}\left(I+\frac{\tilde{A}_n h}{N}\right)^N\right\|_\infty \|\tilde{x}-\tilde{y}\|_\infty \\
&= \lim_{N\to\infty}\left\|I+\frac{\tilde{A}_n h}{N}\right\|_\infty^N \|\tilde{x}-\tilde{y}\|_\infty
\end{aligned}$$

In proving Lemma 2.2.1 we showed that $I+\frac{A_\xi h}{N}$ is element wise positive. This property clearly passes to the submatrix $I+\frac{\tilde{A}_\xi h}{N}$. Hence, in evaluating the matrix norm we can drop the absolute value and we obtain the following inequality.

$$\|e^{A_\xi h}x - e^{A_\xi h}y\| \leq \lim_{N\to\infty}\left(\max_{i\in 1,\ldots,M-1}\sum_{j=1}^{M-1}\left[I+\frac{\tilde{A}_n h}{N}\right]_{i,j}\right)^N \|\tilde{x}-\tilde{y}\|_\infty$$

An arbitrary row i in above sum can take on two possible values, depending on whether the node i is connected to the sink node or not: either $1-\frac{h}{N}\left(\lambda+\gamma\right)$ or $1-\frac{h}{N}\gamma$. Taking the maximum of these terms we can bound the above expression as

$$\begin{aligned}
\|e^{A_\xi h}x - e^{A_\xi h}y\| &\leq \lim_{N\to\infty}\left(1-\frac{h}{N}\gamma\right)^N \|\tilde{x}-\tilde{y}\|_\infty \\
&= e^{-\gamma h}\|x-y\|_\infty
\end{aligned}$$

The last expression follows from the definition of the exponential for scalars and the fact that $\|\tilde{x}-\tilde{y}\|_\infty = \|x-y\|_\infty$ for all $x, y \in S$. Lastly, since $e^{-\gamma h}<1$ for any $\gamma>0$, we conclude that $f_\xi\left(x\right)=e^{A_\xi h}x$ is a contraction mapping and $e^{-\gamma h}$-Lipschitz. $\square$

Using these results we can finally show that (2.6) converges in distribution by using a result of Diaconis in [5]. Suppose f_ξ and K_ξ are as in (2.8). Then,

Theorem 2.2.3. (Diaconis 1998) *Let $(S, \|\cdot\|)$ be a complete separable metric space. Let $\{f_\xi : \xi \in \Xi\}$ be a family of Lipschitz Functions on S, and let μ be a probability distribution on Ξ. Suppose that $\int K_\xi \, \mu(d\xi) < \infty$, $\int \|f_\xi(x_0) - x_0\| \, \mu(d\xi) < \infty$ for some $x_0 \in S$ and $\int \log K_\xi \, \mu(d\xi) < 0$.*

1. *The induced Markov chain has a unique stationary distribution π.*

2. *$\rho[P_n(x, \cdot), \pi] < A_x r^n$ for constants A_x and r with $0 < A_x < \infty$ and $0 < r < 1$, where ρ is the Prokhorov metric [1]. This bound holds for all times n and all starting states x.*

3. *The constant r does not depend on n or x ; the constant A_x does not depend on n, and $A_x < a + b\|x - x_0\|$ where $0 < a, b < \infty$.*

In other words, if the conditions of the theorem are satisfied, the IRM will have a unique stationary distribution π and will converge to the distribution exponentially in the Prokhorov metric ρ. In the context of our problem, the above conditions reduce to

1. $\sum_{\xi \in \Xi} K_\xi p_\xi < \infty$

[1] Let $\mathcal{P}(M)$ denote the collection of all probability measures on the measurable space $(M, \mathcal{B}(M))$. The Prokhorov metric $\rho : \mathcal{P}^2(M) \to [0, +\infty)$ between two probability measures μ and ν is defined as $\pi(\mu, \nu) = \inf\{\varepsilon > 0 \mid \mu(A) \leq \nu(A^\varepsilon) + \varepsilon \text{ and } \nu(A) \leq \mu(A^\varepsilon) + \varepsilon \text{ for all } A \in \mathcal{B}(M)\}$. The ϵ-neighborhood of set A, A^ϵ, is defined as $\cup_{p \in A} B_\epsilon(p)$ – where $B_\epsilon(p)$ is the open ball with radius ϵ centered on p. For details see [2].

2. $\sum_{\xi\in\Xi} ||f_\xi(x_0) - x_0||_\infty p_\xi < \infty$ for some $x_0 \in S$

3. $\sum_{\xi\in\Xi} \log K_\xi p_\xi < 0$

From condition 3 we see that $\log K_\xi < 0$ when $K_\xi < 1$; this encapsulates the idea of the maps f_ξ contracting on average. Substituting our bound $K_\xi = e^{-\gamma h}$ we see that conditions 1 and 3 follow immediately . To prove the second condition, let us select $x_0 = (T, 0, \cdots, 0)$, we see that for this value $||f_\xi(x_0) - x_0||_\infty \leq (M+1)T$ and so this condition follows. We therefore conclude that $\{\theta_n; n \geq 0\}$, constructed by (2.6) converges when the sequence $\{A_n; n \geq 0\}$ is i.i.d.

2.2.2 The Stationary Case

To show that the sequence converges when $\{A_n; n \geq 0\}$ belongs to a more general class of stationary processes we will make use of a lemma by Loynes [14].

Lemma 2.2.4. (Loynes lemma) *Let the random variables $\theta_n (n \geq 1)$ be related by the transformation*

$$\theta_{n+1} = f(\theta_n, A_n), \tag{2.10}$$

where $\{A_n : -\infty < n < \infty\}$ is a stationary sequence. Suppose in addition that $f(x, y)$ is monotonically increasing and continuous from the left (even at ∞) in x, and non-negative.

Then, there exists a stationary sequence of (possibly dishonest) random variables $(\Theta_n : -\infty < n < \infty)$ satisfying

$$\Theta_{n+1} = f(\Theta_n, A_n),$$

such that if $\theta_1 = 0$*, the distribution function of* θ_n *tends monotonically to that of* Θ_0 *as* n *tends to* ∞*. Furthermore,* Θ_n *is the minimal sequence satisfying (2.10) for all* n*, in the sense that if* $\{x_n\}$ *is any other such sequence, then* $x_n \geq \Theta_n$*.*

Using this lemma we can prove the following result.

Theorem 2.2.5. *Suppose* $\{\theta_n; n \geq 1\}$ *is a sequence of random variables related by (2.6) with the initial condition that* $\theta_1 = 0$*. Suppose, moreover, that* $\{A_n; n \geq 1\}$ *is a stationary sequence of random matricies of the form (2.5). Then,* $\theta_n \to \Theta_0$ *in distribution, where* Θ_0 *is some random variable.*

Proof. (Theorem 2.2.5) We can exclude the possibility that Θ_0 is dishonest since the vectors θ_n are bounded from above by T. The result follows directly from the Loynes lemma, therefore we show that the conditions of the lemma are satisfied, i.e.,

$$f(\theta_n, A_n) = e^{A_n h}\theta_n$$

is monotonically increasing and positive in θ_n. In the context of Euclidean space, increasing and positive are interpreted as element-wise, i.e., if $\theta \geq \phi$ for each element of θ and ϕ, then

$$e^{A_n h}\theta \geq e^{A_n h}\phi$$

or equivalently that $e^{A_n h}(\theta - \phi) \geq 0$. Since $(\theta - \phi) \geq 0$ a sufficient condition that f is monotonically increasing is that $e^{A_n h}$ is element-wise non-negative. However, this is the result of Lemma 2.2.1, and the theorem follows. □

To drop the condition in the above lemma that $\theta_1 = 0$, we show that the limiting distribution is independent of the initial distribution. Specifically, it is possible to show that, given two initial temperature vectors, $\phi_0, \theta_0 \in S$, then $\|\phi_n - \theta_n\|_\infty \to 0$. When this is true, we say that the limiting distribution is *stable* with respect to the initial conditions. We begin the demonstration by writing the evolution of the difference as,

$$\phi_{n+1} - \theta_{n+1} = \left(\prod_{k=0}^{n} e^{A_k h} \right) (\phi_0 - \theta_0)$$

Using the fact that the first term of $\phi_0 - \theta_0$ is zero and the form of the matrix exponential in (2.7), it is clear that the first term of $\phi_{n+1} - \theta_{n+1}$ is zero for all n. Moreover, it is also clear that the first term of the difference provides no contribution to the evolution of the other terms. To show that the norm goes to zero, it is then only necessary to consider again the $(1,1)$-submatrix. We can continue the development as follows,

$$\begin{aligned} \|\phi_{n+1} - \theta_{n+1}\|_\infty &\leq \left|\left| \prod_{k=0}^{n} e^{A_k h} \right|\right|_\infty \|\phi_0 - \theta_0\|_\infty \\ &\leq \left(\prod_{k=0}^{n} \left|\left| e^{A_k h} \right|\right|_\infty \right) \|\phi_0 - \theta_0\|_\infty \end{aligned}$$

We can now make use of the bound found in the proof of Lemma 2.2.2 to write

$$\begin{aligned} \|\phi_{n+1} - \theta_{n+1}\|_\infty &\leq \left[\prod_{k=0}^{n} \lim_{N\to\infty} \left(1 - \frac{h}{N}\gamma\right)^N \right] \|\phi_0 - \theta_0\|_\infty \\ &= e^{-nh\gamma} \|\phi_0 - \theta_0\|_\infty \end{aligned}$$

Allowing $n \to \infty$, we see that $\|\phi_{n+1} - \theta_{n+1}\|_\infty \to 0$ as required.

2.3 The Average Temperature for Homogeneous Nodes with an Ergodic Temperature Process.

If in addition to assuming that the connectivity process of nodes is stationary, we also assume that the non-sink nodes are homogeneous, in the sense that they share a common mobility pattern, and that the temperature is ergodic, in the sense that the time average of the temperature process converges to the ensemble average, it is possible to derive the nodes mean temperature in the following way.

For any non-sink node, we can write the temperature dynamics as follows:

$$\theta_i(n+1) = (1-\gamma h)\theta_i(n) + h\sum_{j=1}^{N} \lambda C_{ji}(n)\left[\theta_j(n) - \theta_i(n)\right] + h\lambda C_{0i}(n)\left[T - \theta_i(n)\right]$$

Taking the expectation of both sides we can write

$$\begin{aligned} E\left[\theta_i(n+1)\right] &= (1-\gamma h)E\left[\theta_i(n)\right] \\ &\quad + h\sum_{j=1}^{N} \lambda E\left[C_{ji}(n)\right]\left(E\left[\theta_j(n)\right] - E\left[\theta_i(n)\right]\right) \\ &\quad + h\lambda E\left[C_{0i}(n)\right]\left(T - E\left[\theta_i(n)\right]\right) \end{aligned}$$

Since nodes sharing the same mobility pattern, would also have the same average temperature, we can set $E[\theta_i(n)] = E[\theta_j(n)]$. Moreover, from our result that the temperature vector converges in distribution, in the steady state we can write that $E[\theta_i(n+1)] = E[\theta_i(n)] = \mu_{\theta_i}$. Simplifying the above expression we can then obtain,

$$\mu_{\theta_i} = \frac{\lambda T E[C_{0i}(0)]}{\gamma + \lambda E[C_{0i}(0)]} \tag{2.11}$$

This is an intuitively satisfying result. Indeed, we see that if the non-sink nodes did not lose heat to the environment ($\gamma = 0$), their average temperature would approach that of the sink node. The results of this calculation are shown in some of the simulations in the next chapter for homogeneous nodes that follow an i.i.d and Markov connectivity model.

Chapter 3

Simulations

To visualize the dynamics of the model and assess the accuracy of the above analysis we set up four simulations. The first simulation assumes that the connectivity between nodes is governed by an independent identically distributed (i.i.d) Bernoulli random processes. At each epoch of time, two nodes are connected with a probability p that is independent of its connectivity at previous time epochs and disconnected with a probability $1 - p$. This simple connectivity model will allow us to see the effects of the various parameters in the model on the overall steady-state temperature distribution of the nodes.

The second simulation will add an additional level of complexity by using a Markov connectivity model. A Markov model will allow us to simulate additional properties of ad-hoc networks. In particular, the connectivity of nodes from one epoch to the next are not independent; a node in contact with another node may be more likely to remain in contact with that node in the next time epoch, and likewise, a node that is not in contact with a another node is likely to remain not in contact at the next time epoch. For both the i.i.d and Markov connectivity models, we will simulate one hour worth of dynamics in time steps of 0.1 seconds and allow connectivity changes every 10 seconds. The empirical mean is calculated from the last 50% of the samples. This will allow the dynamics to reach a steady state.

The third and fourth simulations will employ a Random Waypoint (RWP) mobility model. The RWP model has been extensively studied and is used extensively in mobile networking research. In the first of the RWP simulations we will assume that mobility is homogeneous, in the sense that all the nodes share the same domain of mobility as well as other parameters of the RWP model. The second RWP simulation will introduce heterogeneity by varying the domain of the nodes as well as furnishing the nodes with mobility parameters in a manner to be discussed below.

In the fifth simulation we will introduce a new, mean-reverting, mobility model based on the Ornstein-Uhlenbeck random process. We will then observe the performance of the algorithm using this new mobility model.

For each of these simulations we will assume that there are 9 nodes, including the sink node. The sink node is maintained at a notional temperature of 100 while the non-sink nodes are initially at a temperature of zero.

3.1 Results using an i.i.d connectivity model.

Figures 3.1 and 3.2 show the dynamics and steady-state distribution of temperature of a typical node for various values of p , λ and γ when the connectivity between nodes are a i.i.d-Bernoulli as described above.

It is apparent that the empirical average temperature of the nodes, shown in the figure as the green line labeled as μ_{hat}, does indeed correspond to the value theory expects from equation (2.11). The theoretically expected temperature is

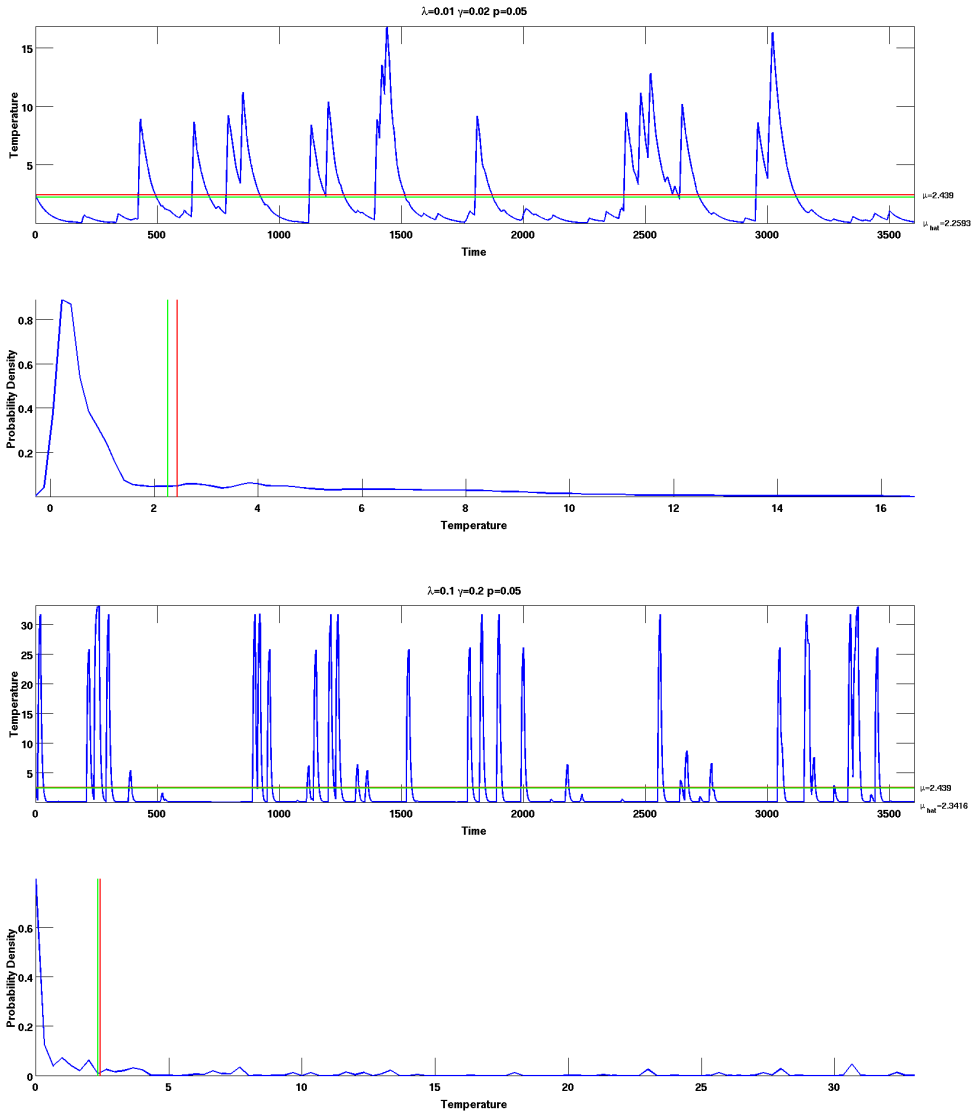

Figure 3.1: Temperature distribution of nodes using an independent identically distributed (i.i.d) Bernoulli connectivity model with $p = 0.05$.

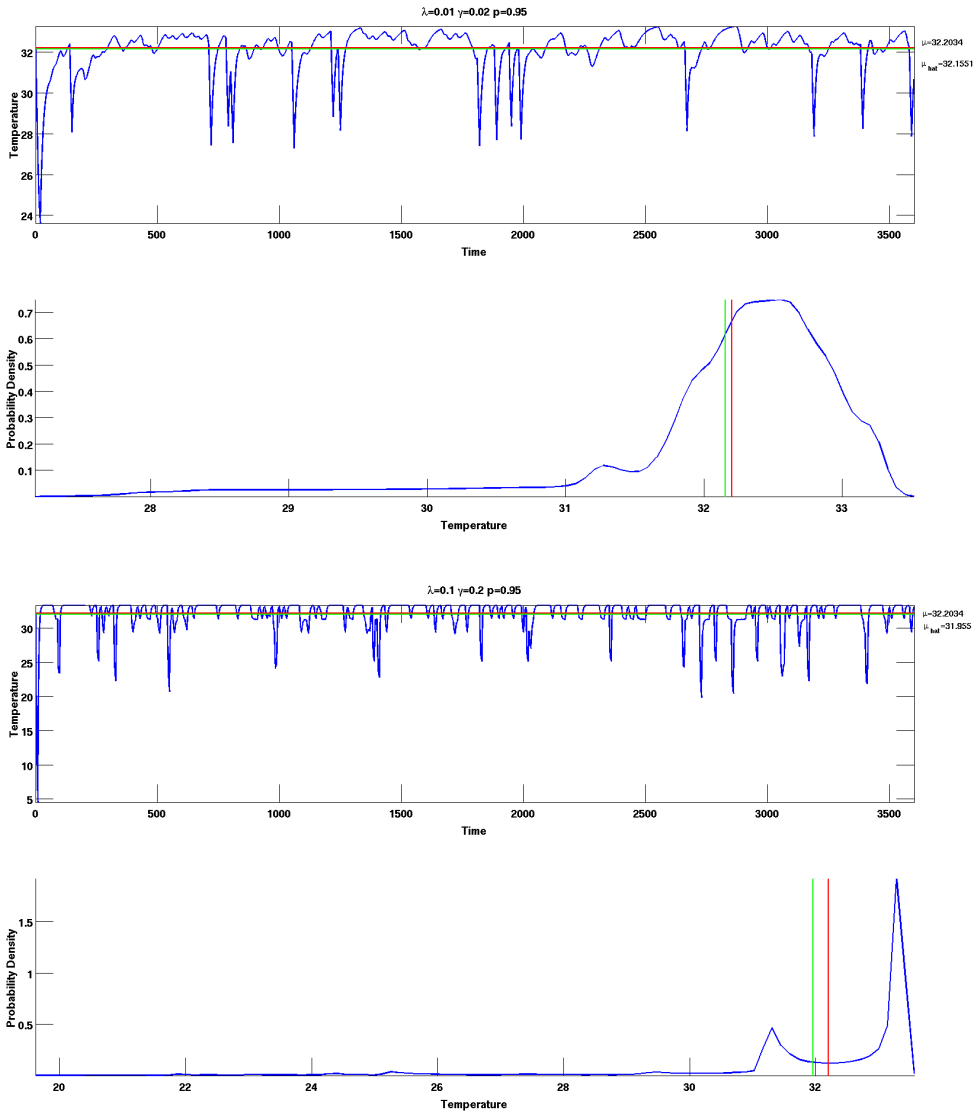

Figure 3.2: Temperature distribution of nodes using an independent identically distributed (i.i.d) Bernoulli connectivity model with $p = 0.95$.

shown as the red line labeled as μ. Naturally as p increases, the average temperature increases; commensurate with increased exposure to the sink node. The effect of the heat transfer coefficients λ and γ are also visible. We observe that as these values are increased, in the i.i.d setting, the volatility of the temperature increases. This behavior is reasonable since nodes would both lose heat to the environment more quickly as well as gain heat from the source node and other nodes more quickly.

3.2 Results using a Markov connectivity model.

A Markov connectivity model, for the reasons described previously, would represent a next step in producing a realistic connectivity process. Specifically, this model assumes that the pair-wise connectivity between two nodes is governed by a Markov random process. Figure 3.3 is a graphical representation of this model. The values of p and q can be tuned to values that can serve as proxies for connectivity characteristics. For example, it is elementary to show that expected number of epochs during which two nodes would be connected or disconnected would be given by $\frac{1}{(1-q)}$ and $\frac{1}{(1-p)}$, respectively. It is also straight forward to show that the probability that two nodes would be connected or disconnected is given by $\Pi_c = \frac{(1-p)}{(1-p)+(1-q)}$ and $\Pi_d = \frac{(1-q)}{(1-p)+(1-q)}$, respectively. Using these calculations, and the fact that $E[C_{0i}(0)] = \Pi_c$, we can also derive the expression for the mean temperature as follows

$$\mu_{\theta_i} = \frac{\lambda T \frac{(1-p)}{(1-p)+(1-q)}}{\gamma + \lambda \frac{(1-p)}{(1-p)+(1-q)}}$$

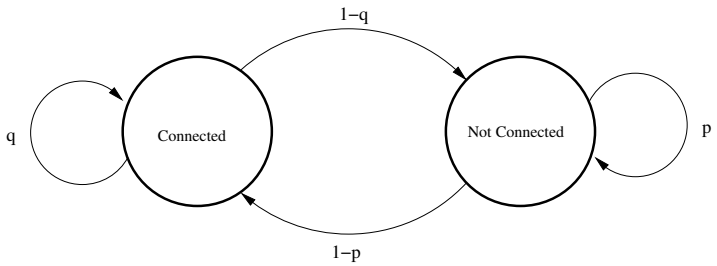

Figure 3.3: Markov connectivity model.

Figures 3.4 and 3.4 shows the temperature evolution of a typical node for various values of λ, γ, p and q. We see immediately that the Markov connectivity model possesses a greater diversity of behavior than is present in the i.i.d model. We observe the effects of sustained periods of connectivity and detachment from the sink node as evidenced by the sustained periods of exponential growth and decay. Indeed, we also observe that for particular values of p and q, that the stationary distribution of temperature can be bimodal, a feature missing from the i.i.d case.

3.3 Results using a Random Way Point mobility model.

The RWP model is used extensively in mobile networking research. In basic outlines, the model starts with a number of nodes distributed over a subset of $\mathbb{R}^2$. Each node then selects a destination within this domain and a speed within some interval $[v_{min}, v_{max}]$. The node then travels to the selected destination at the selected speed. Once it arrives at the destination it rests for a period T_{rest} and the process then iterates. First used by Johnson and Maltz [8] in the study of ad-hoc source routing algorithms, the model has become extensively studied in its own right. It has been shown, for example, that contrary to intuition, for any interval where

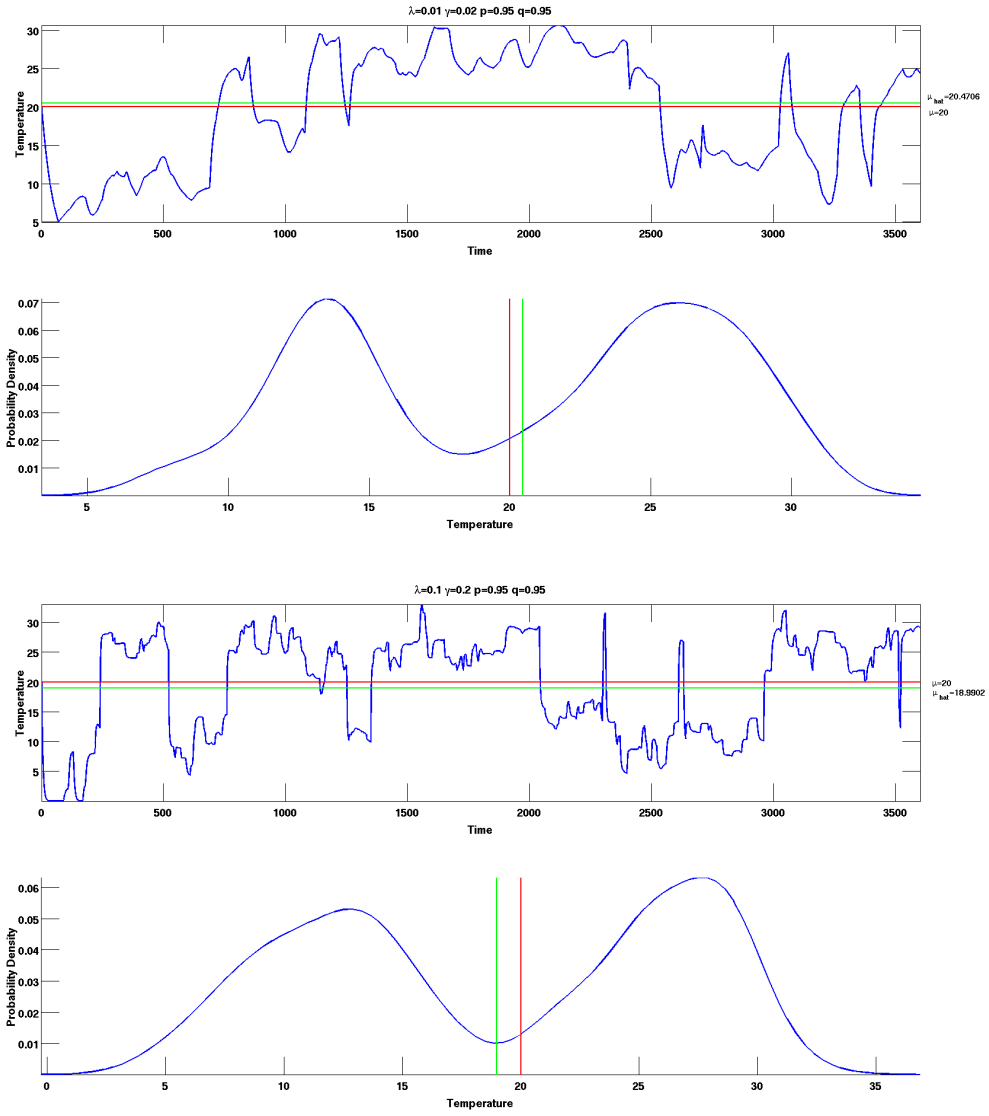

Figure 3.4: Temperature distribution of nodes using a Markov connectivity model with $p = 0.95$ and $q = 0.95$

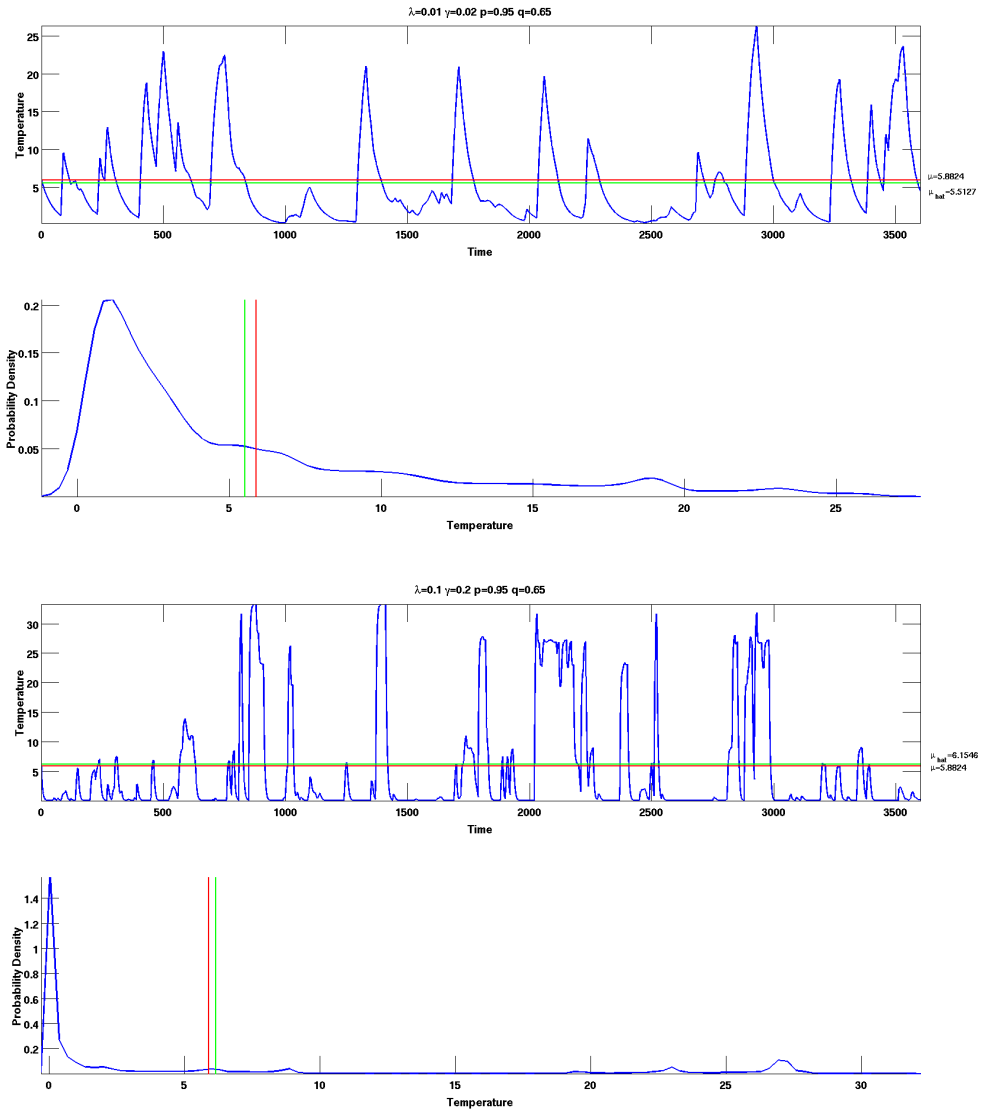

Figure 3.5: Temperature distribution of nodes using a Markov connectivity model with $p = 0.95$ and $q = 0.65$

$v_{min} = 0$, the nodes do not move around with average velocity $v_{max}/2$. Instead, it converges to zero, i.e., the nodes eventually become stationary [22]. A number of results regarding the steady-state distribution of the nodes [11] as well as a number of connectivity properties of this model have also become available [1].

Our motivation for using RWP is to observe the performance of the algorithm using a well known mobility model as well as to investigate the effects of heterogeneous mobility on the performance of the proposed algorithm. To do this we present two simulations, the first with a homogeneous mobility pattern and the second with heterogeneous mobility pattern. In both case, we simulate 9 nodes moving on a square, 100 square mile area. This would imply an average node density of 0.1 nodes / square mile ; or conversely 10 square miles per node. Since we want the network to be disconnected most of the time, we chose a maximum communication radius of 1 miles $< \sqrt{10}$ miles. In the homogeneous case, the nine nodes use the entire simulation space, and their speeds are selected from the interval [30 mph, 60 mph].In the heterogeneous case, we segregate the nodes evenly into three overlapping subsets of the simulation space. The first subset of nodes occupy a square area from $(0, 0)$ to $(4, 4)$, the second subset from $(2, 2)$ to $(8, 8)$ and the last from $(6, 6)$ to $(10, 10)$. In the first and third domain the nodes select their velocities from the interval [10 mph, 30 mph] while in the second the nodes velocities are selected from the interval [30 mph, 60 mph]. One can envision this as modeling high speed nodes in less populated areas ferreting messages between slower moving nodes in more densely populated areas. For both simulation, we also rather arbitrarily, select $\lambda = 1$ and $\gamma = 0.001$. Figures (3.6) and (3.7) show the results

of these simulations for the homogeneous and heterogeneous cases, respectively. In both figures, the color of the node corresponds to its temperature. The location of the nominal message is shown as a '□' on the plot and the sink node is shown slightly larger than the rest of the nodes.

In the homogeneous case of Figure (3.6), between plots (a) and (b), the sink node moves in a north easterly direction from near the origin, while the message carrying node begins moving in a north westerly direction from the lower right of the graph. From plots (b) and (c) we see that that the message is transferred to a warmer intermediary, having been exposed to the sink node earlier. The sink node in the meantime has moved rapidly to the upper right. Between plots (c) and (d) we observe the new intermediary moving from the lower left to the the vicinity of the sink node in the upper right. Between (d) and (e) we see that the message is transferred yet again to a warmer intermediary and lastly in plot (f) we see that the message is successfully delivered after 13055 seconds or roughly 3.6 hours. While in this simulation, the message was delivered as expected in a straight forward manner, other runs of the simulation presented several unexpected pathologies. For example, messages would occasionally be passed to warmer nodes that were moving *away* from the sink node. If this node was moving at high speed, this would result in the message being carried far from the sink node. Other times, messages would be passed to warmer nodes that were moving very slowly, when it, perhaps, would have been more advantageous for the node to retain the message for a different node in the future.

In the heterogenous case of Figure (3.7), the initial source of the message was

chosen randomly among the nodes in the third subdomain and the sink was selected randomly from the nodes of the first subdomain. In figure (a) we can clearly see the segregation of the nodes into the three subdomains. From (a) to (b) on the plot we see that the node containing the message is moving from the upper left to the lower right. Simultaneously, other nodes have been exposed to the sink and have commensurately warmed up. Between figures (b) and (c), the message carrying node from the third subdomain comes into contact with a warmer node from the second subdomain, having gained indirect exposure to the sink node, and subsequently transfers its message to this new intermediary. Likewise, from (c) to (d) we notice that the node containing the message becomes exposed to a node hotter than it within the *same* subdomain and transfers its message to it. From (d) to (e) the message is ferried to within the vicinity of the first subdomain and lastly, on plot (f) we see that the message has been successfully passed to the sink node in 10125 seconds or roughly 2.8 hours.

The significant improvement in the delivery latency between the homogeneous and heterogeneous cases, which has been evident over repeated simulations, can be explained by the fact that heterogeneous nodes carry with them more information about their surroundings and interactions than their homogeneous counterparts. In a homogeneous environment, since one node is the same as another, there is no reason to expect that it would perform any better in delivering packets to the sink node. Heterogeneous mobility on the other hand, results in varying abilities among the nodes in their ability to deliver packets and hence manifests itself in the meaningful diversity of temperatures with the proposed algorithm utilizes in its

routing decisions.

3.4 An Ornstein-Uhlenbeck mobility model

Like the RWP, another common model that has been used in mobile networking research, more for its simplicity than its accuracy, is the Random Walk (RW). Under the RW model, nodes follow a Brownian motion trajectory; over each simulation time step Δt, the node selects the next increment in each spatial direction from the normal random variable $\sigma\sqrt{\Delta t}\mathcal{N}(0,1)$, where σ is the volatility. The RW model has an infinite domain and, in the two dimensional and higher setting, will almost surely never return to the origin. This is contrary to an evidence of significant mean reversion found in empirical mobility studies and from basic reasoning that, in general, people and machines eventually return to home bases.

In this thesis, we introduce a new mobility model related to the RW, that with only slightly additional complication allows us to simulate this mean-reverting behavior. This mobility model, replaces the simple Brownian Motion of the RW with trajectories derived from an Ornstein-Uhlenbeck (OU) random process. The OU process can be thought of as a filtered Brownian motion or as a mean reverting Brownian motion and can be expressed as the stochastic differential equation (SDE)

$$dX_t = \theta(\mu - X_t)\,dt + \sigma dB_t$$

where B_t is a standard Brownian Motion, $\sigma \geq 0$ the volatility, μ the mean and $\theta \geq 0$, a measure of the processes' central tendency. If we momentarily suppress the

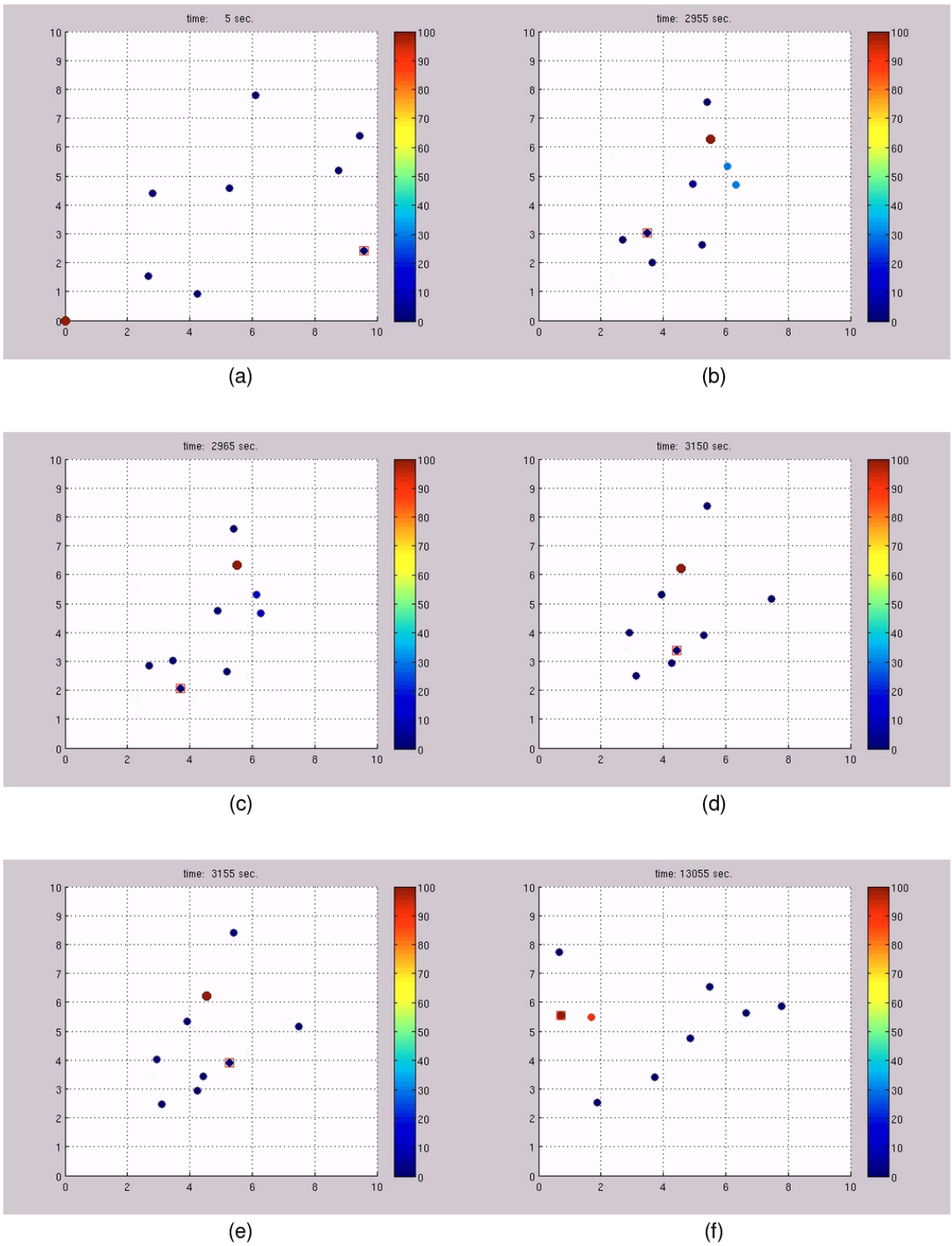

Figure 3.6: Message passing using thermodynamic algorithm on a Random Waypoint mobility model in a homogeneous mobility setting.

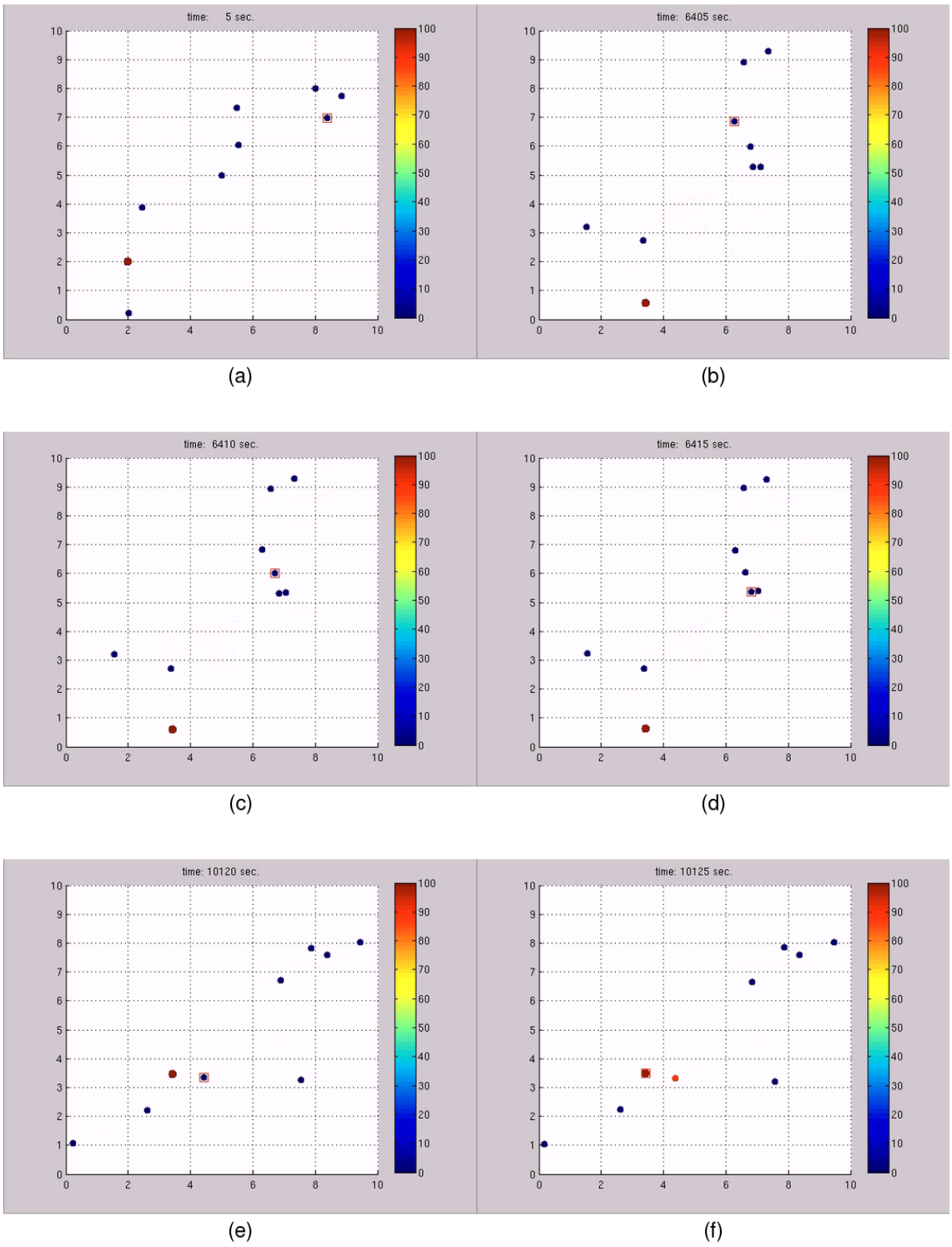

Figure 3.7: Message passing using thermodynamic algorithm on a Random Waypoint mobility model in a heterogenous mobility setting.

the random component of the above SDE, by setting $\sigma = 0$, we see why this process is mean reverting; if $X_t > \mu$ then $\frac{dX_t}{dt} < 0$ implying a downward tendency towards μ, while the opposite is true if $X_t < \mu$. In fact the solution of this now deterministic ordinary differential equations is

$$X_t = \mu\left(1 - e^{-\theta t}\right) + X_0 e^{-\theta t}$$

and we see that as $t \to \infty$, $X_t \to \mu$ exponentially with a rate θ. Because of this mean reverting property, this process has, historically, been used to model several mean reverting phenomena including interest rates and commodity prices. A general solution to the the SDE is obtained by an application of Ito's lemma [15]

$$X_t = X_0 e^{-\theta t} + \mu\left(1 - e^{-\theta t}\right) + \sigma\sqrt{\frac{1 - e^{-2\theta t}}{2\theta}}\mathcal{N}(0, 1)$$

We see that in the steady state, when $t \to \infty$, the distribution of nodes following an OU process converges to a normal distribution centered about μ with variance $\frac{\sigma^2}{2\theta}$. We can tune the statistical properties of our mobility model by selecting the appropriate values of μ, σ and θ.

3.4.1 Results using an OU mobility model

For our simulations, we vary the mean reverting tendency μ and compute σ so that we attain a desired standard deviation for the nodes (i.e., the square root of the variance.) A single standard deviation encompasses roughly 68% of samples, while two standard deviations encompass roughly 95% of samples. Therefore, tuning the

standard deviation of the nodes allows us to model the average spread of nodes in the simulation. For our simulation we selected a standard deviation of 1, by using a $\theta = 0.05$ and a corresponding $\sigma \approx 0.316$. Since a new direction is chosen for each node at every time step, the trajectories of the nodes are naturally more jagged than is the case with the RWP model. Figure 3.8 shows the results of our simulation. We see that for these values, the message has been delivered to the sink node in roughly 10 minutes. This has been consistent across a number of repeated simulations.

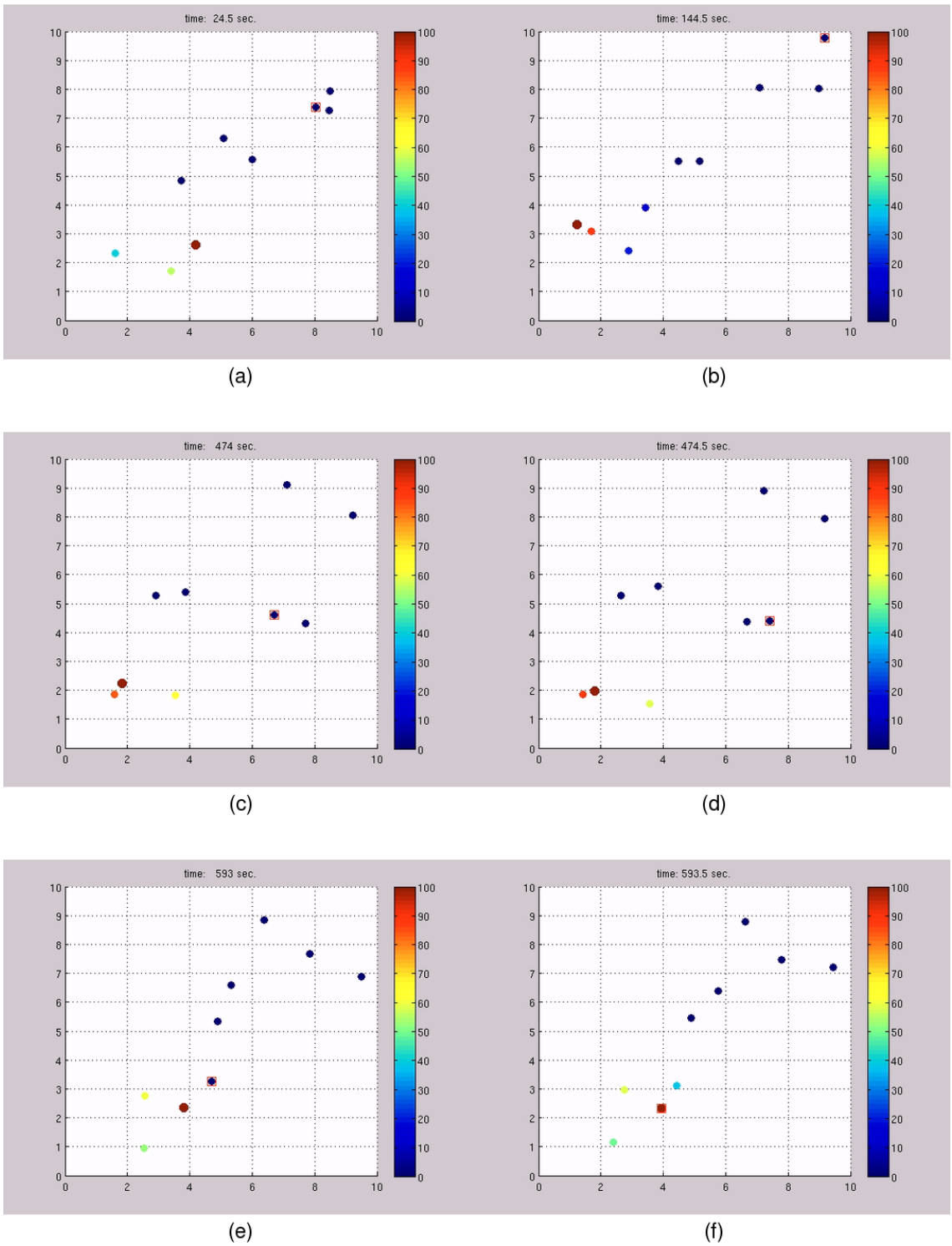

Figure 3.8: Message passing using thermodynamic algorithm on a Ornstein-Uhlenbeck mobility model.

Chapter 4

Conclusions and Future Work

4.1 Conclusion

In this thesis, we established the convergence in norm and distribution of the temperature vector of a new thermodynamically inspired routing algorithm for DTN networks, derived an expression for the mean temperature of the steady-state distribution in the stationary case, and simulated the proposed algorithm on a number of mobility models. Through these simulations, we have demonstrated that the algorithm successfully achieves its objective of delivering messages to the sink node, and performs particularly well in heterogeneous environments. There are, however, a number of directions this research can be expanded, both to understand additional properties of the proposed algorithm, as well as to suggest possible improvements.

From a theoretical perspective, there are several interesting problems that can be asked. While we have established that the algorithm is stable, in the sense that the temperature vectors converge to a unique stationary distribution under a stationary connectivity assumption, perhaps the most important measure of performance is how efficiently the algorithm routes messages from source to destination. In this regard, it would be useful to derive an estimate of the expected latency under various connectivity models. While this is likely to be intractable for most connectivity models, it may be possible to attempt to find bounds for simple connectivity models

like the i.i.d. case. Moreover, while we have established convergence in the discrete case, convergence in the general continuous time case remains open. As mentioned in the introduction, a possible attack towards this problem may be the discovery of a common quadratic Lyapunov function over all possible heat transfer matrices.

From a practical standpoint, it would be interesting to examine the effect of combining any of the replication schemes described in Section 1.2 to the delivery performance of the algorithm. In particular, it may be advantageous to replace the Delivery Likelihood (DL) metric of MaxProp given by Equation (1.1) by our simpler thermodynamic metric. This would have the advantage of continuing to measure the indirect exposure of nodes to the sink nodes, while obviating the need for complicated maximum probability path computations.

Another possible direction for improvement of the basic algorithm, derives from observing the performance of the algorithm on the RWP and OU mobility models. A common pathology present in these simulation was that messages would be passed to nodes, that though warmer than their previous carriers, were moving *away* from the destination and often at the same time the original carrier was moving *towards* the destination. This motivates an idea that in addition to the absolute temperature of the nodes, the second derivative of the temperature with respect to time might be a useful metric in making routing decisions, i.e., if the node is getting hotter or colder with time. By discriminating along this second metric, it may be possible that the algorithm will show improved performance in homogeneous settings where this pathology was most commonly observed, or as the message carrier nears the vicinity of the sink node where other possible carriers are likely have a similar

range of temperatures.

The thermodynamically inspired routing algorithm for DTN networks, presented here, has engendered a number of interesting problems, a few of which have been answered in this thesis. It is hoped that work on this algorithm will continue and eventually find an application on deployed systems.

Appendix A

An Alternative Derivation of the Matrix Exponential Function.

For any square matrix A, We want to show the equality of

$$\lim_{N\to\infty}\left(I+\frac{A}{N}\right)^N=\sum_{k=0}^{\infty}\frac{A^k}{k!}$$

We do this by showing that

$$\lim_{N\to\infty}\left|\left|\sum_{k=0}^{\infty}\frac{A^k}{k!}-\left[I+\frac{A}{N}\right]^N\right|\right|=0$$

We begin by splitting the sum in the first term to yield the following sequence of inequalities

$$\begin{aligned}
\lim_{N\to\infty}\left|\left|\sum_{k=0}^{\infty}\frac{A^k}{k!}-\left[I+\frac{A}{N}\right]^N\right|\right| &= \lim_{N\to\infty}\left|\left|\sum_{k=0}^{N}\frac{A^k}{k!}-\left[I+\frac{A}{N}\right]^N+\sum_{k=N+1}^{\infty}\frac{A^k}{k!}\right|\right| \\
&\leq \lim_{N\to\infty}\left|\left|\sum_{k=0}^{N}\frac{A^k}{k!}-\left[I+\frac{A}{N}\right]^N\right|\right|+\left|\left|\sum_{k=N+1}^{\infty}\frac{A^k}{k!}\right|\right| \\
&\leq \lim_{N\to\infty}\left|\left|\sum_{k=0}^{N}\frac{A^k}{k!}-\left[I+\frac{A}{N}\right]^N\right|\right|+\sum_{k=N+1}^{\infty}\frac{||A||^k}{k!}
\end{aligned}$$

Since it is clear that the second term goes to zero as $N\to\infty$, it is only left to show that the first term also goes to zero. The binomial expression in the first term can be expanded using the binomial formula, as follows

$$\begin{aligned}\left[I+\frac{A}{N}\right]^N &= \lim_{N\to\infty}\sum_{k=0}^{N}\binom{N}{k}\left(\frac{A}{N}\right)^k I^{N-k} \\ &= \sum_{k=0}^{N}\frac{N!}{k!\,(N-k)!}\frac{A^k}{N^k} \\ &= \sum_{k=0}^{N}\frac{N!}{N^k\,(N-k)!}\frac{A^k}{k!} \\ &= \sum_{k=0}^{N}\left[\prod_{l=0}^{k-1}\left(1-\frac{l}{N}\right)\frac{A^k}{k!}\right]\end{aligned}$$

Substituting this formula into the previous expression we obtain

$$\begin{aligned}\lim_{N\to\infty}\left|\left|\sum_{k=0}^{N}\frac{A^k}{k!}-\left[I+\frac{A}{N}\right]^N\right|\right| &= \lim_{N\to\infty}\left|\left|\sum_{k=0}^{N}\left[1-\prod_{l=0}^{k-1}\left(1-\frac{l}{N}\right)\right]\frac{A^k}{k!}\right|\right| \\ &\leq \lim_{N\to\infty}\sum_{k=0}^{N}\left[1-\prod_{l=0}^{k-1}\left(1-\frac{l}{N}\right)\right]\frac{||A||^k}{k!} \\ &= \lim_{N\to\infty}\sum_{k=0}^{N}\frac{||A||^k}{k!}-\lim_{N\to\infty}\sum_{k=0}^{N}\left[\prod_{l=0}^{k-1}\left(1-\frac{l}{N}\right)\right]\frac{||A||^k}{k!}\end{aligned}$$

To show that the above limit is zero, we prove that the second term is identical to the first. This can be established using a sequence of functions

$$f_N(k)=\begin{cases}\prod_{l=1}^{k-1}\left(1-\frac{l}{N}\right) & \text{if } k\leq N \\ 0 & \text{if } k>N\end{cases}$$

We see that for any $k\in\mathbb{Z}_+$, $f_N(k)$ is uniformly bounded by 1. Moreover, we note that $\sum_{k=0}^{\infty}\frac{||A||^k}{k!}=e^{||A||}\leq\infty$. Combined, we can then make use of the bounded convergence theorem to interchange the order of sum and limit, i.e. ,

$$\begin{aligned}\lim_{N\to\infty}\sum_{k=0}^{\infty} f_N(k)\frac{||A||^k}{k!} &= \lim_{N\to\infty}\sum_{k=0}^{N}\left[\prod_{l=0}^{k-1}\left(1-\frac{l}{N}\right)\right]\frac{||A||^k}{k!} \\ &= \sum_{k=0}^{\infty}\lim_{N\to\infty} f_N(k)\frac{||A||^k}{k!} \\ &= \sum_{k=0}^{\infty}\frac{||A||^k}{k!}\end{aligned}$$

and the equality is established. It follows that

$$\lim_{N\to\infty}\left|\left|\sum_{k=0}^{\infty}\frac{A^k}{k!}-\left[I+\frac{A}{N}\right]^N\right|\right|=0$$

and equality is proved.

Bibliography

[1] Muhammad Abdulla and Robert Simon. Characteristics of common mobility models for opportunistic networks. In *PM2HW2N '07: Proceedings of the 2nd ACM workshop on Performance monitoring and measurement of heterogeneous wireless and wired networks*, pages 105–109, New York, NY, USA, 2007. ACM.

[2] Patrick Billingsley. *Convergence of Probability Measures*. John Wiley & Sons, 1999.

[3] John Burgess, Brian Gallagher, David Jensen, and Brian Neil Levine. Maxprop: Routing for vehicle-based disruption-tolerant networks. In *In Proc. IEEE INFOCOM*, 2006.

[4] S. Burleigh, A. Hooke, L. Torgerson, K. Fall, V. Cerf, B. Durst, K. Scott, and H. Weiss. Delay-tolerant networking: an approach to interplanetary internet. *IEEE Communications Magazine*, 41(6):128–136, 2003.

[5] Persi Diaconis and David Freedman. Iterated random functions. *SIAM Rev.*, 41(1):45–76, 1999.

[6] Arshad Islam and Marcel Waldvogel. Reality-check for dtn routing algorithms. In *ICDCSW '08: Proceedings of the 2008 The 28th International Conference on Distributed Computing Systems Workshops*, pages 204–209, Washington, DC, USA, 2008. IEEE Computer Society.

[7] Sushant Jain, Kevin Fall, and Rabin Patra. Routing in a delay tolerant network. In *SIGCOMM '04: Proceedings of the 2004 conference on Applications, technologies, architectures, and protocols for computer communications*, pages 145–158, New York, NY, USA, 2004. ACM.

[8] David B. Johnson and David A. Maltz. Dynamic source routing in ad hoc wireless networks. In *Mobile Computing*, pages 153–181. Kluwer Academic Publishers, 1996.

[9] Philo Juang, Hidekazu Oki, Yong Wang, Margaret Martonosi, Li Shiuan Peh, and Daniel Rubenstein. Energy-efficient computing for wildlife tracking: design tradeoffs and early experiences with zebranet. *SIGOPS Oper. Syst. Rev.*, 36(5):96–107, 2002.

[10] Mehdi Kalantari and Richard J. La. A dtn packet forwarding scheme inspired by thermodynamics.

[11] Pasi Lassila. Spatial node distribution of the random waypoint mobility model with applications. *IEEE Transactions on Mobile Computing*, 5(6):680–694, 2006. Member-Hyytia, Esa and Member-Virtamo, Jorma.

[12] Yong Liao, Kun Tan, Zhensheng Zhang, and Lixin Gao. Estimation based erasure-coding routing in delay tolerant networks. In *IWCMC '06: Proceedings of the 2006 international conference on Wireless communications and mobile computing*, pages 557–562, New York, NY, USA, 2006. ACM.

[13] John R. Liukkonen and Arnold Levine. On convergence of iterated random maps. *SIAM J. Control Optim.*, 32(6):1752–1762, 1994.

[14] R. M. Loynes. The stability of a queue with non-independent inter-arrival and service times. *Mathematical Proceedings of the Cambridge Philosophical Society*, 58(03):497–520, 1962.

[15] Bernt Oksendal. *Stochastic Differential Equations: An Introduction with Applications*. Springer, sixth edition, 2003.

[16] Wilson J. Rugh. *Linear System Theory*. Information and System Sciences Series. Prentice Hall, 2nd edition, 1996.

[17] Thrasyvoulos Spyropoulos, Konstantinos Psounis, and Cauligi S. Raghavendra. Spray and wait: an efficient routing scheme for intermittently connected mobile networks. In *WDTN '05: Proceedings of the 2005 ACM SIGCOMM workshop on Delay-tolerant networking*, pages 252–259, New York, NY, USA, 2005. ACM.

[18] Gilbert Strang. *Linear Algebra and Its Applications*. Brooks Cole, February 1988.

[19] Zhendong Sun and Shuzhi Sam Ge. *Switched Linear Systems: Control and Design*. Communications and Control Engineering. Springer, March 2005.

[20] Amin Vahdat and David Becker. Epidemic routing for partially-connected ad hoc networks. Technical report, 2000.

[21] Yong Wang, Sushant Jain, Margaret Martonosi, and Kevin Fall. Erasure-coding based routing for opportunistic networks. In *WDTN '05: Proceedings of the 2005 ACM SIGCOMM workshop on Delay-tolerant networking*, pages 229–236, New York, NY, USA, 2005. ACM.

[22] J. Yoon, M. Liu, and B. Noble. Random waypoint considered harmful. In *Proceedings of the 22nd Annual Joint Conference of the IEEE Computer and Communications Societies (INFOCOM)*, volume 2, pages 1312–1321, April 2003.